PAUL SCHERRER INSTITUT

SWISS LIGHT SOURCE SLS

SLS-TME-TA-2004-0244
3rd May 2004

100 keV Gun Test Stand: Design and Parameter Study

Simon C. Leemann

Paul Scherrer Institut, CH-5232 Villigen PSI, Switzerland

Abstract

In the scope of the LEG Project [1] a field emitter array (FEA) cathode is being considered as an electron source. In order to study the emission of electrons from such a cathode and to study space charge compensation techniques as well as to develop diagnostic procedures to characterize the beam resulting from such a setup it has been decided to build a 100 keV gun test stand. Such a test stand gun has been modeled in 2D with the code MAFIA [2] and an extensive parameter study has been conducted. The results of this parameter study are presented and consequences for the design and operation of the test stand are derived.

1 Design of the 100 keV Test Stand

In August 2003 a proposal for a 100 keV test stand was written [3]. In brief, the motivation behind building such a test stand is to deliver a characterization of the electron beam emerging from a field emitter array (FEA) source (phase space distribution, emittance, energy spread, charge) and to investigate emittance minimization techniques. In order to compare different anode/cathode designs and emittance minimization schemes the test stand was required to have a modular design.

In such a design the test stand consists of a permanent part containing the HV power supplies, vacuum pumps, controls, and other necessary infrastructure as well as a ”flexible” part containing the removable gun electrodes, solenoid magnet, beam pipe, and diagnostic devices.

In this note we will focus on the ”flexible” part. The permanent part will be considered as a black box capable of delivering pulsed DC voltage up to -100 kV to the cathode with respect to the grounded anode as well as providing vacuum pressure of roughly 10^{-8} mbar within the gun and beam pipe. The two modular parts of the setup are connected by a 300 mm long ceramic structure that surrounds the cathode mount and acts as a HV insulator.

The ”flexible” part is made up of a CF200 cube (6-way chamber) attached to a piece of beam pipe. The diagnostics module can be driven through this beam pipe. The cube holds the anode mount and solenoid structure and it offers access for the primary pump. The remaining three ports are used for additional diagnostic devices (Faraday cup, slit masks, screen).

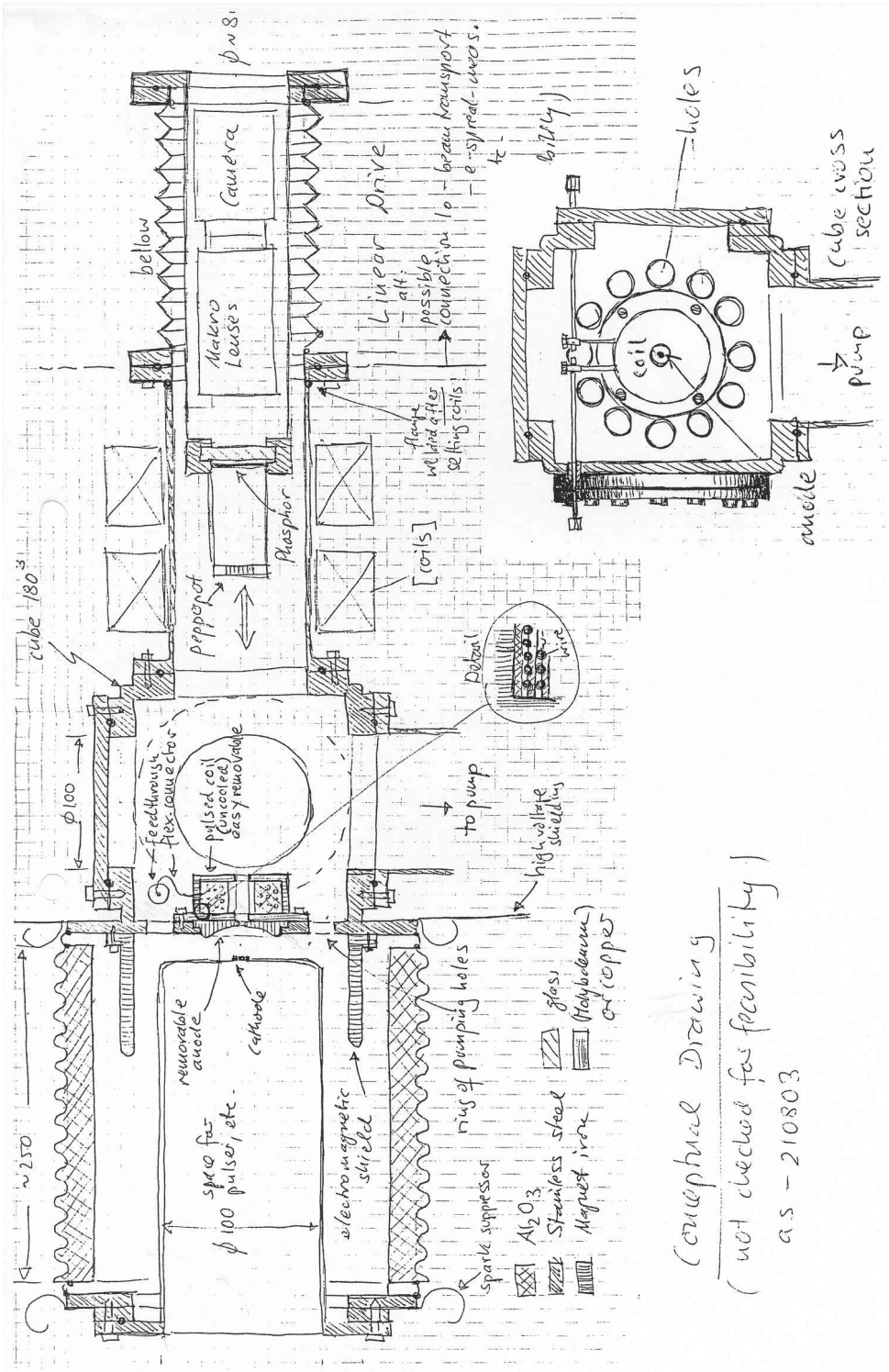

Figure 1: Conceptual drawing showing the ceramic insulator with the removable cathode, the cube with the anode mount and solenoid, the beam pipe, and the diagnostics module [3].

2 Gun Design

Starting with a simple design suggestion [4] we began to evaluate electrode configurations. Due to the design of the mounts the space for the electrodes was limited to a radius of 30 mm and a length of 50 mm. Within these limits we tried to optimize the design in order to deliver minimal emittance at the exit of the gun structure. Additional constraints are that no particles should be lost at or behind the anode iris and that the resulting electrical field strength remains below 20 MV/m [5] at all surfaces in order to avoid arcs.

On the cathode an area with r = 0.5 mm was left untouched as it is foreseen to install the FEA at this location. The actual FEA (with an active emitter area radius of r_{act} = 100 μm) will be attached to the top of a transistor-like structure which will in turn be clamped to the back of the cathode plate in such a manner that its surface is in the same plane as the surrounding electrode material.

2.1 A Simple Design Example

A first design is shown in figure 2. The peak electrical field strength is observed at the tip of the anode.[1] This is undesirable, but in principal it can not fully be avoided.[2] An improvement can be made by enlarging the curvature radius of this tip in order to reduce the local field strength. However, while doing so one has to take care that the distance to any part of the cathode structure remains as large as possible in order to keep the global field strength sufficiently low. Such an attempt will be discussed in the next section.

The anode has been recessed in the vicinity of the beam axis to make sure that outer beam particles do not collide with the anode structure after passing the iris. In the example seen in figure 2 this anode geometry allows a bunch with a 100 mA peak current to pass the diode structure without losing any particles at the iris or on the anode material (see also sections 3.3 and 3.4). Since the field strength downstream of the iris is negligible due to the screening effect of the anode structure, this recess can be enlarged if necessary in order to achieve higher current without particle loss.

Away from the anode tip, the electric field strength is fairly relaxed. The field seen by the accelerated electrons depends exclusively on the local geometry regardless of modifications made outside the gap area. The resulting field strengths are determined primarily by the length of the gap between the cathode and the anode tip. In the example shown in figure 2 the gap has been chosen so that the peak electric field strength remains below 20 MV/m. However, if this gap is varied the expected 1/r behavior is

[1] When modeling the gun structure one has to take care that the underlying grid specified in the MAFIA input file is chosen in a manner that resolves the entire geometry sufficiently. However for such fine structures, this can lead to very long run time ($\sim$10 h).

[2] This holds true even in the simplest case of a two-plate diode structure where the anode has a small hole allowing the electrons to pass. Along the edge of this iris the same behavior mentioned above will be encountered (see section 2.2).

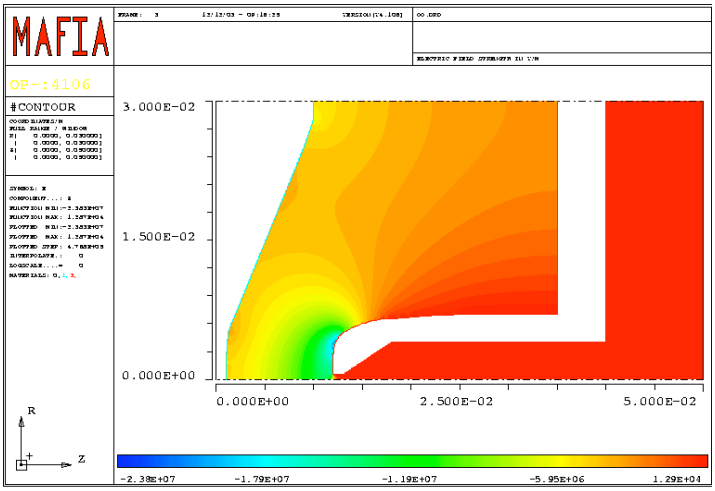

Figure 2: A simple electrode configuration (cathode on the left, anode on the right) capable of emitting a 100 keV electron beam with a normalized transverse emittance of $1.8 \cdot 10^{-7}$ m·rad. The color scale refers to the electrical field strength in V/m; dimensions of the geometry are given in m. The peak electrical field strength is 19 MV/m and is found to be at the anode tip (colored blue).

encountered as demonstrated in figure 3. If vacuum conditions and materials allow, the gap can be closed to reach higher field strengths which can lead to a lower emittance as will be demonstrated in section 3.2.

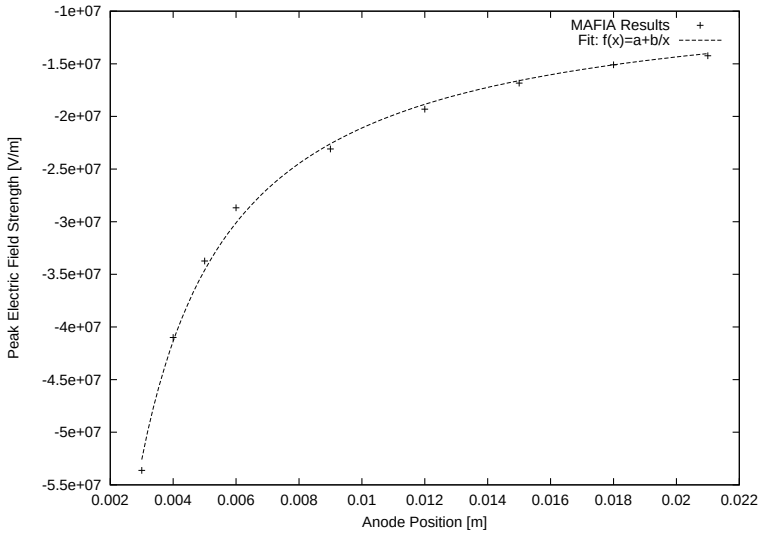

Figure 3: MAFIA simulation of the resulting peak electrical field strength when varying the gap between the cathode and anode structures of the design shown in figure 2. The expected 1/r behavior is apparent.

2.2 An Improved Design

It has been suggested [6] that only the peak and not the mean electric field strength is a critical parameter, due to the fact that breakdown (and consequently possible damage to the FEA or the electrodes) occurs after a single arc regardless of the exact location of the arc within the structure. Such an arc would be expected at the location of peak electric field strength which is at the anode iris. Therefore, the design of the outer parts of the electrodes can be simplified to arbitrary extent as long as the resulting surface electric field strength is lower than at the anode iris.

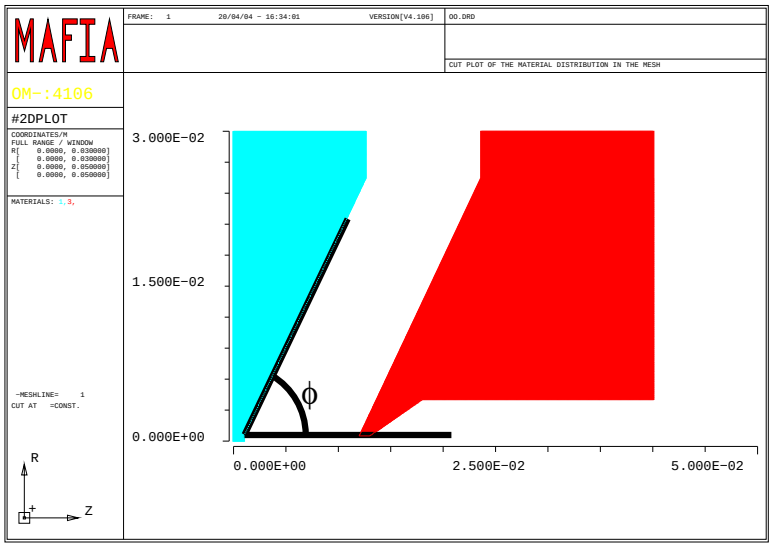

Figure 4: A simplified gun geometry: the cathode electrode is on the left (blue), the anode on the right (red). The tilt angle of the cathode electrode is labeled.

Additionally, the cathode electrode (around the area reserved for the FEA structure) has a tilt which makes the resulting electrostatic field inherently focussing (the electric field lines are perpendicular to the equipotential cathode surface). However, this tilt angle has to be chosen carefully to avoid over-focussing of the beam. Figure 4 shows the simplified geometry and the angle determining this tilt. According to [7] selecting the so-called ”Pierce angle” of 67.5° would deliver parallel flow in a cylindric beam. Ideally one wants to select the angle that delivers minimal transverse emittance at the end of the gun (beam focus); therefore one would expect to need an angle which is smaller than the Pierce angle. Figure 5 shows the resulting emittance at the end of the gun for different cathode electrode tilt angles while keeping the gap distance constant. It appears a cathode electrode tilt angle of 65° delivers the minimum emittance at the gun exit. Choosing larger angles will increase emittance, although a perfectly vertical cathode electrode (tilt angle 90°) does not render maximum emittance; the maximum emittance is found at 75°. Below 60° particles will be lost on the cathode electrode itself! The optimized design with 65° tilt angle is shown in figure 6; the resulting peak electrical field strenght is 19 MV/m.

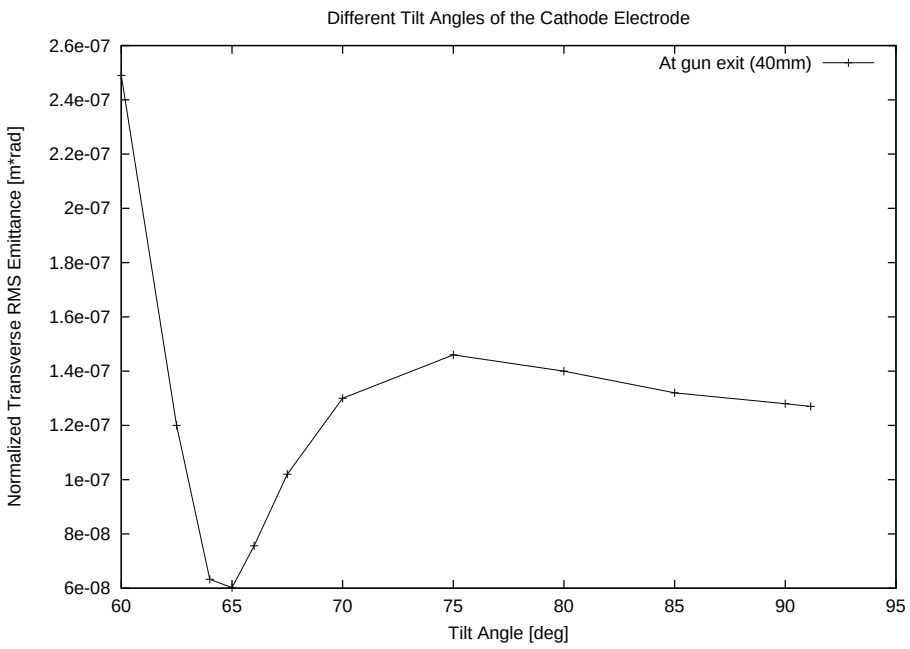

Figure 5: Resulting emittance at the gun exit for different tilt angles of the cathode electrode surrounding the FEA; minimum emittance is achieved at 65°.

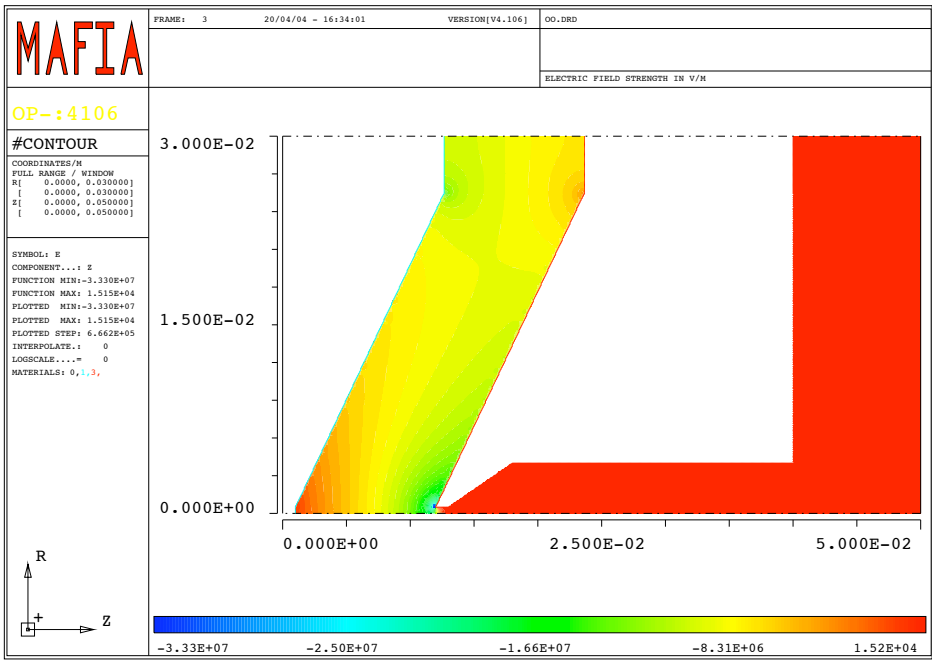

Figure 6: An improved gun geometry suggestion. The normalized transverse emittance has been reduced to $6{\cdot}10^{-8}$ m·rad at the exit of the gun; the peak electrical field strength is 19 MV/m.

3 Parameter Studies

In the following parameter studies the passage of a bunch of electrons through the gun introduced in section 2.1 has been simulated. In addition to the accelerating diode structure the solenoid magnet has been included as well as an 280 mm long drift section. The setup is depicted in figure 7.

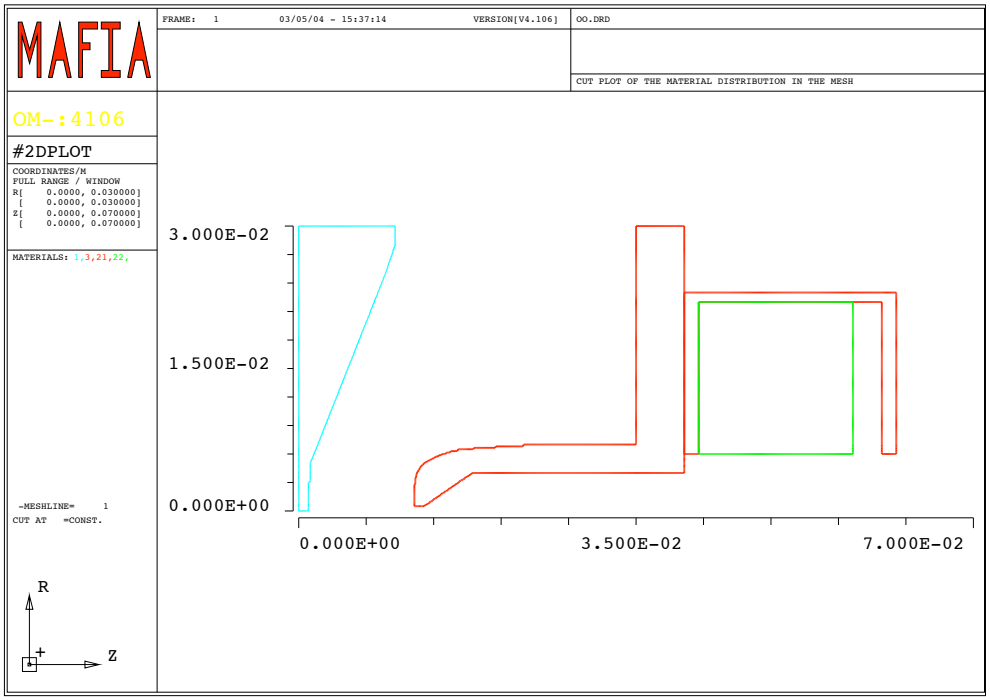

Figure 7: The simulated section: cathode, anode, and solenoid magnet. The 280 mm drift following the solenoid magnet structure is not displayed in this diagram.

The following list summarizes the relevant parameters used in the MAFIA input file.

- Cathode potential: -100 kV
- Active emitter radius: r_{act} = 100 μm
- Pulse: Gaussian, cut-off at $\pm 3\sigma_t$, σ_t = 20 ps, Q = -5.0133·10^{-12} C ($\hat{I}$ = 100 mA)
- Initial energy: $\gamma_0 = 1.0001$, initial divergence is set to zero
- Iris: r_{iris} = 500 μm
- Tracked macro-particles: N = 20000
- Tracked path: From the cathode surface at z_0 = 1 mm to the end of the drift section at z = 342 mm

In order to calculate the total charge Q_b contained in a Gaussian bunch with a certain peak current $\hat{I}$ it is useful to recall:

$$I(t) = \hat{I} \cdot e^{-\frac{(t-t_0)^2}{2\sigma^2}} \tag{1}$$

Where the total charge contained within the bunch is:

$$Q_b = \int_{-\infty}^{+\infty} I(t)\, dt \tag{2}$$

Which defines the relationship between bunch charge and peak current:

$$\hat{I} = \frac{Q_b}{\sqrt{2\pi} \cdot \sigma} \tag{3}$$

3.1 Solenoid Field

A solenoid magnet has been designed [8] in order to create a beam focus at a location within the CF200 cube (see section 1). As shown in figures 1 and 7 the solenoid magnet consists of water-cooled Cu tubes as windings (with a total cross-section of 16 mm $\times$ 16 mm) enclosed in a steal yoke of 17 mm width and 22 mm length. This solenoid coil has a maximum current flux of 5.4 A/mm^2. According to MAFIA simulations this gives an peak on-axis magnetic field of $B_z \simeq 85$ mT as can be seen in figure 8.

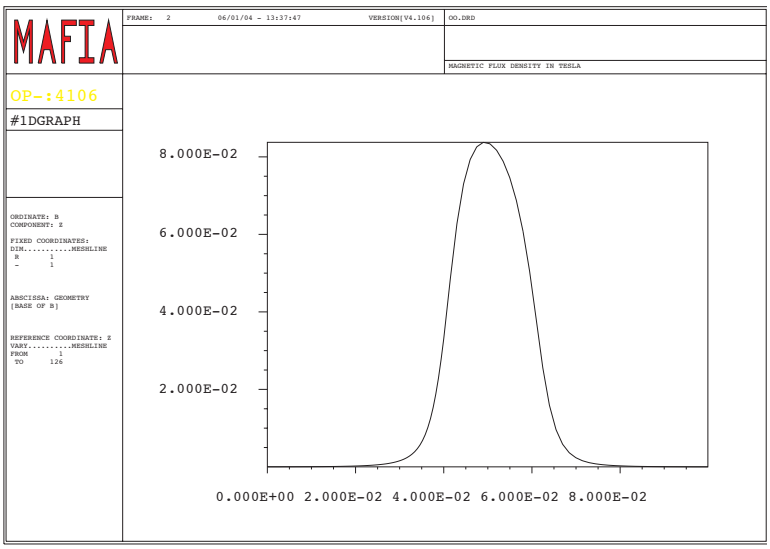

Figure 8: The solenoid magnet structure simulated with MAFIA: magnetic field on axis in T vs. longitudinal position in m.

Figure 9 compares normalized transverse emittances for a turned on and turned off solenoid. The solenoid strongly blows up the radial emittance while the bunch passes

the solenoid structure, but it reduces the radial emittance for the rest of the path by a factor 2–3. The bunch length increases if solenoid current is applied as can be seen in figure 10.

A comparison of phase spaces for a bunch with and without solenoid focussing shows the expected effect (figure 11). The bunch is compressed by roughly a factor 10 both in radius and radial momentum; the longitudinal phase space is rotated by applying the solenoid [9].

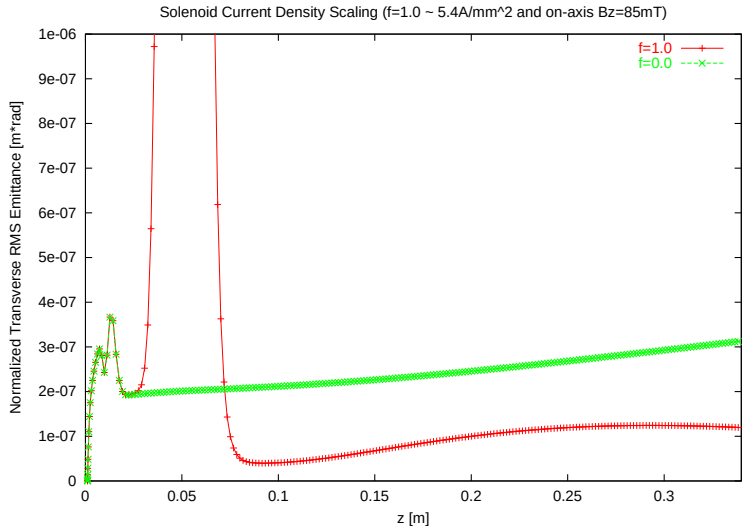

Figure 9: Comparison of normalized transverse emittance with and without solenoid focussing.

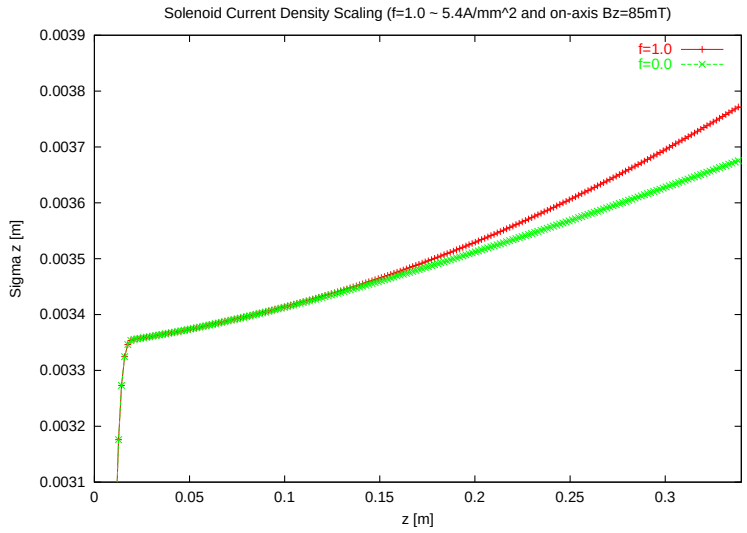

Figure 10: Comparison of bunch length σ_z with and without solenoid focussing.

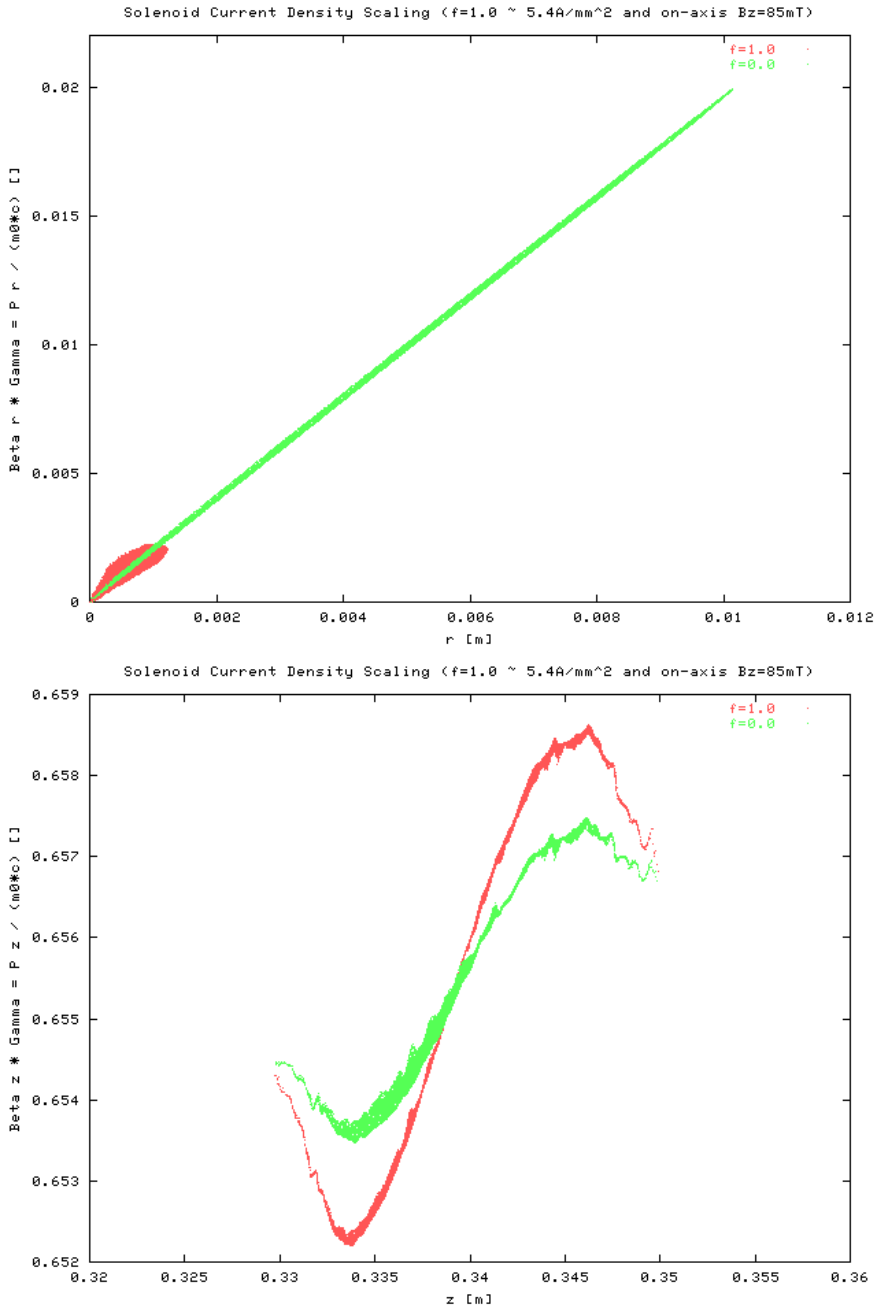

Figure 11: Comparison of the bunch's phase space at the end of the beam line (z = 34 cm) with and without solenoid focussing. Positions are in m and momenta are normalized: $\beta_{r,z}\gamma = p_{r,z}/m_0c$.

As mentioned in the beginning of this section the goal is to focus the beam at a certain location downstream of the solenoid. In figure 9 one can see that such a focus is achieved at z $\simeq$ 10 cm, but one can also assume that there is another focus further

downstream z $>$ 35 cm. Therefore the challenge will be to adjust the solenoid current in such a manner that the focus occurs at the exact location desired. In figure 12 the transverse normalized emittance at the end of the beam line has been plotted vs. the solenoid current scaling. The minimum is obtained for a current scaling factor of f = 1.05. In other words if the focus of the beam is required at the location of end of the beam line, the solenoid current has to be scaled with a factor 1.05. Once the test stand is operational and diagnostic equipment is inserted at a certain location, this procedure can be used to acquire the proper solenoid current value needed to focus the beam at the desired position. An example for different solenoid current scalings, the resulting emittance minima, and their longitudianl location is given in figure 13.

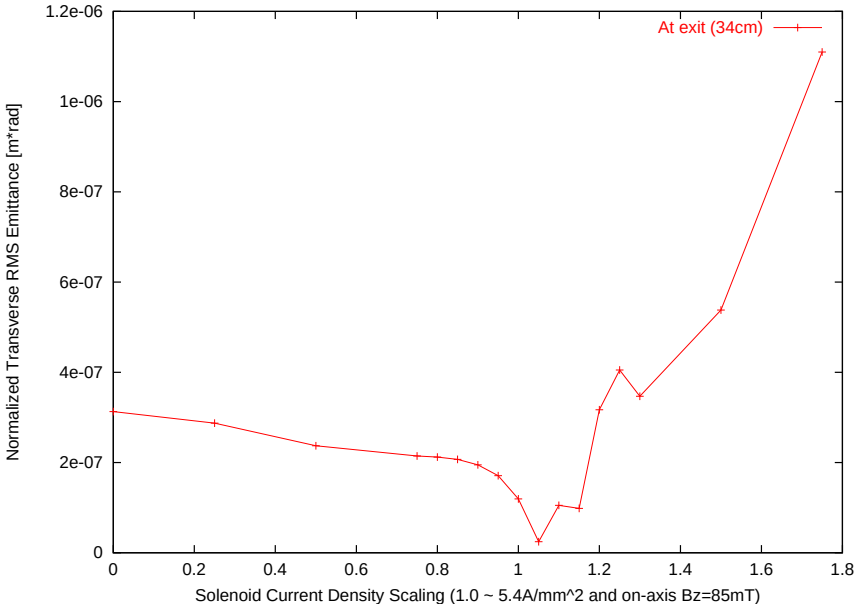

Figure 12: Scaling of the solenoid current in order to find a setting for minimum transverse emittance at the end of the beam line. The minimum is reached with a scaling of f = 1.05.

3.2 Diode Gap

As has been suggested at the end of section 2.1, if vacuum and material conditions allow the gap between the cathode and the anode can be minimized in order to reach higher electric field strength. Clearly arcs causing HV breakdown have to be avoided and therefore maximum electric field strength and ultimately gap distance is limited. The challenge is to approach this limit as close as possible without exceeding it. The advantage of having high accelerating gradients is that the bunch reaches relativistic energies faster which means that non-linear space charge forces (that scale like γ^{-2}) act on the bunch only in a short time window leading to less emittance blow-up. Fig-

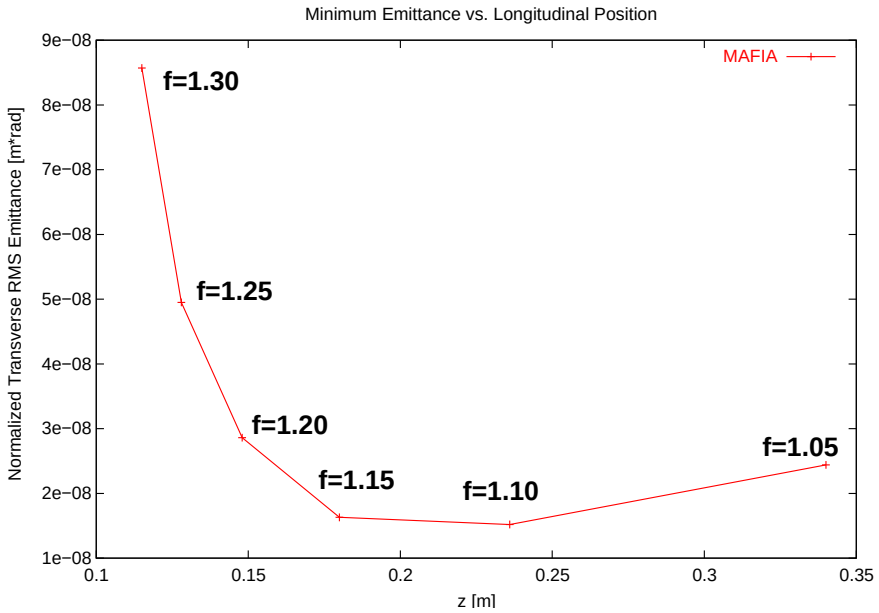

Figure 13: The minimum emittance and its longitudinal position for different solenoid current scalings; f = 1.0 corresponds to a peak longitudinal magnetic field of $B_z \simeq 85$ mT.

ure 14 shows the results of MAFIA simulations for the emittance after passing the drift section for different scalings of solenoid focussing.

It is interesting to note that the original working point with a gap of 11 mm is the maximum gap length that shows no particle loss. If larger gaps are chosen the space charge effects are able to blow up the beam enough so that particles are lost on the anode iris. Shorter gaps have been evaluated here. While the emittance decreases strictly monotonic if no solenoid focussing is applied, the behavior changes as soon as the solenoid current is increased: here the emittance increases when the gap is closed at first until it reaches a local maximum at a gap length of roughly 9 mm from where it will then decrease again to levels slightly lower than those achieved with a 11 mm gap. Assuming that the solenoid magnet is turned on and working at nominal current this means that no emittance benefit can be achieved by closing the gap by only 1–3 mm; in order to get a lower emittace after the drift section, one would have to close the gap by more than 4 mm, which (according to figure 3) corresponds to a peak electric field strength of over 30 MV/m!

Assuming that the anode iris could be machined with a larger diameter, one can try to extrapolate the behavior of the emittance for gap lengths larger than 11 mm. It appears that for large solenoid strengths it would indeed make sense to open the gap in order to achieve a lower emittance after the 30 cm long drift section. However, this behavior depends strongly on the drift length as can be recognized in figure 13.

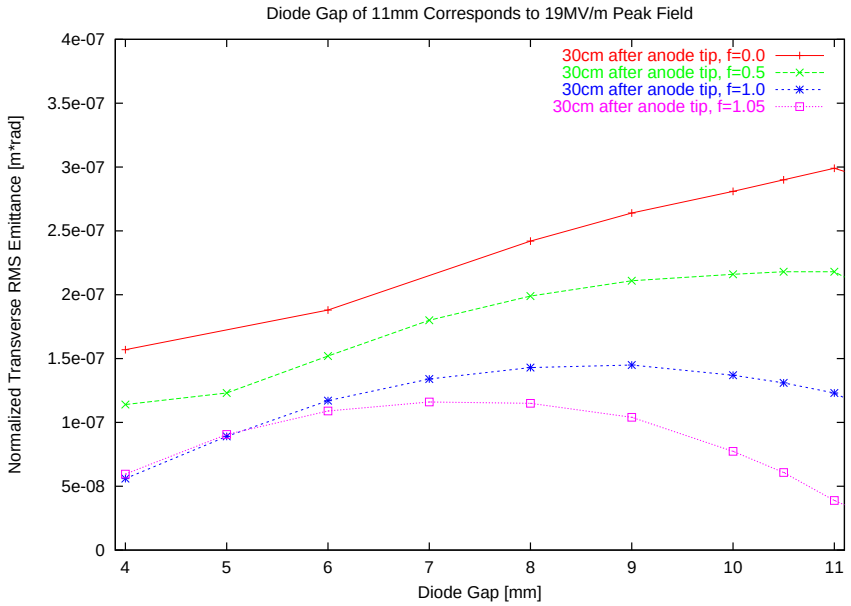

Figure 14: Emittance after a 30 cm drift depending on gap length for four different solenoid scalings; f = 1.0 corresponds to a peak longitudinal magnetic field of $B_z \simeq 85$ mT. If the gap is longer than 11 mm particles are lost on the anode iris.

3.3 Bunch Charge

Another parameter that can be varied is the charge within the bunch. It has been observed that inserting more charge into the bunch than at the original working point (Q = -5.0133·10^{-12} C, $\hat{I}$ = 100 mA) leads to particle loss on the anode iris due to the increased space charge blow-up of the bunch. However, one can reduce the amount of charge within a bunch and observe the influence on the emittance after the bunch has passed the drift section. The results are shown in figure 15 for four different solenoid current scalings.

Without any solenoid focussing there is indeed a non-linear growth of emittance when increasing the charge as one would expect. However, once one introduces solenoid focussing the emittance growth shows linear dependence on the charge contained in the bunch. If the solenoid focussing is scaled by 1.05 (where minimum emittance at the end of the beam line is observed) the emittance shows no more charge dependency. It is interesting to observe that depending on the solenoid focussing strength the character of the charge dependency of the emittance changes so strongly.

3.4 Bunch Length

The simulated bunch is Gaussian with a cut-off at $\pm 3\sigma_t$ where originally σ_t = 20 ps was chosen (see section 4 for more details on this choice of bunch length). The parameter σ_t has been varied for different solenoid focussing strengths in order to compare the

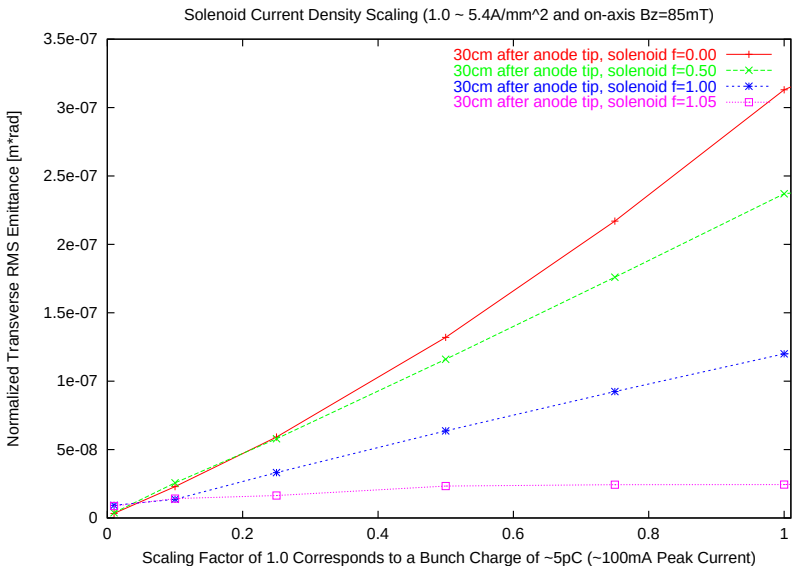

Figure 15: Emittance at the end of the beam line depending on the amount of charge contained in the bunch for four different solenoid scalings; f = 1.0 corresponds to a peak longitudinal magnetic field of $B_z \simeq 85$ mT. A charge scaling factor of 1.0 corresponds to Q = -5.0133·10^{-12} C or a peak current of $\hat{I}$ = 100 mA.

resulting emittance at the end of the test stand beam line. The results are shown in figure 16.

As expected increasing the bunch length leads to a smaller emittance due to the decreased space charge forces. It has been observed that scaling factors lower than 1.0 resulted in particle losses at the anode iris. This again reflects the fact the chosen working point renders a bunch which has maximum charge density with respect to the anode iris geometry; increasing the charge density leads to stronger space charge forces and thus to an excessive emittance blow up. Additionally it is interesting to note that for a solenoid strength scaling factor of 1.0 or above figure 16 suggests there is a minimum emittance, whereas for solenoid scaling 0.0 and 0.5 the emittance decreases with the increase of the bunch length. For a solenoid scaling of 1.0 the emittance is minimal for a bunch length scaling of roughly 8. For a solenoid scaling of 1.05 this minimum is approached for a bunch length scaling of roughly 3.

3.5 Active Emitter Area

In section 2 it has already been mentioned that the actual FEA will be a very small area attached to the top of a transistor-like mounting structure. This circular emitting surface is expected to have a radius of r_{act} = 100 μm, however depending on the results of current studies this radius could change in the future. Therefore the resulting emittance at the end of the test stand beam line has been simulated depending on different radii of the FEA. This is displayed in figure 17.

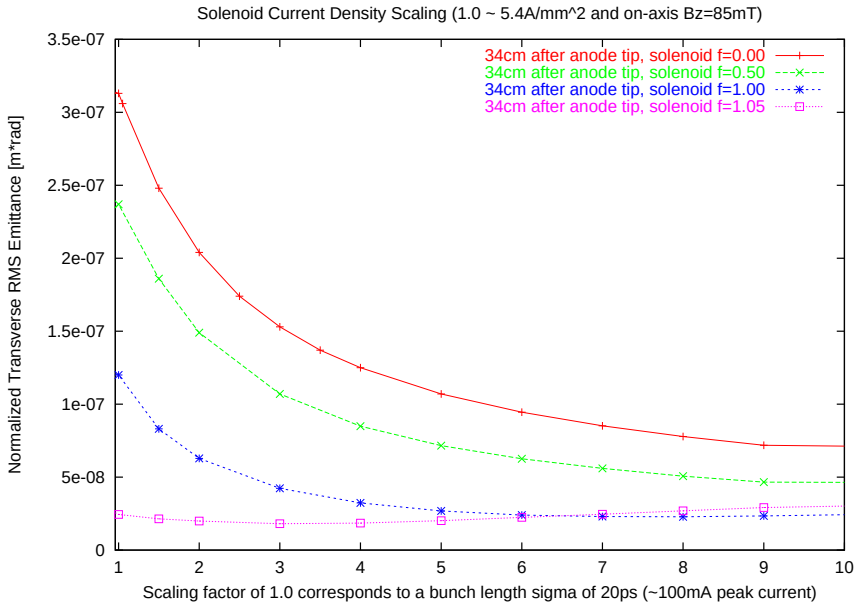

Figure 16: Emittance at the end of the beam line depending on the bunch length for four different solenoid scalings; f = 1.0 corresponds to a peak longitudinal magnetic field of $B_z \simeq 85$ mT. A bunch length scaling factor of 1.0 corresponds to σ_t = 20 ps.

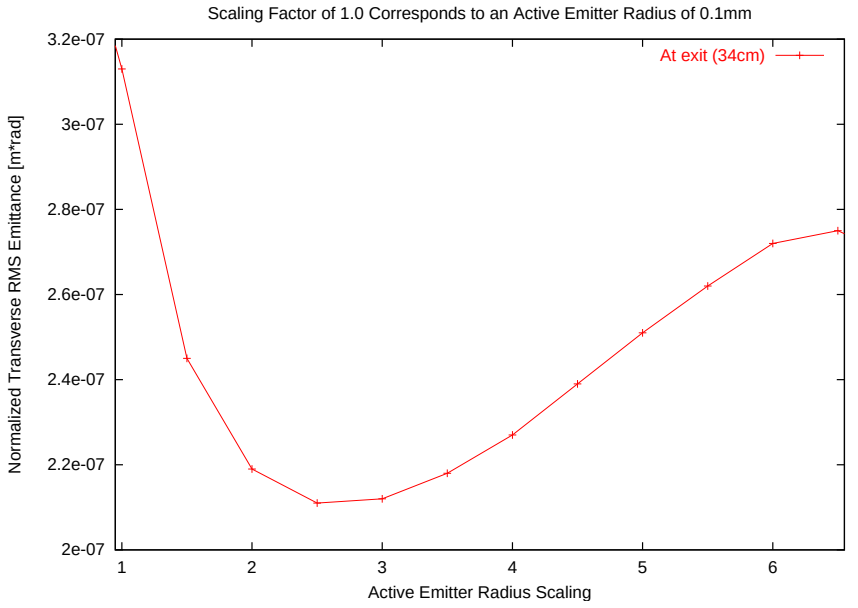

Figure 17: Emittance at the end of the beam line depending on the radius of the active emitter area. An active emitter radius scaling factor of 1.0 corresponds to r_{act} = 100 μm.

Clearly there is an emittance minimum (although the resulting absolute reduction in emittance is no more than $\simeq 10^{-7}$ m·rad) for a radius scaling of roughly 2.5. This emittance minimum is the result of choosing the proper ratio between emitter radius and anode iris radius thus leading to an optimum electro-static focussing force. In the final test stand setup a specific FEA will be given. Therefore it will be necessary to simulate the resulting emittance depending on the anode iris radius in order to find the minimal emittance achievable with a certain FEA. With the present active emitter area of r_{act} = 100 μm the chosen anode iris radius is the smallest radius that will allow the full 100 mA peak current bunch to pass without particle loss. As shown in figure 18 it is also the radius that delivers the smallest emittance at the end of the gun.

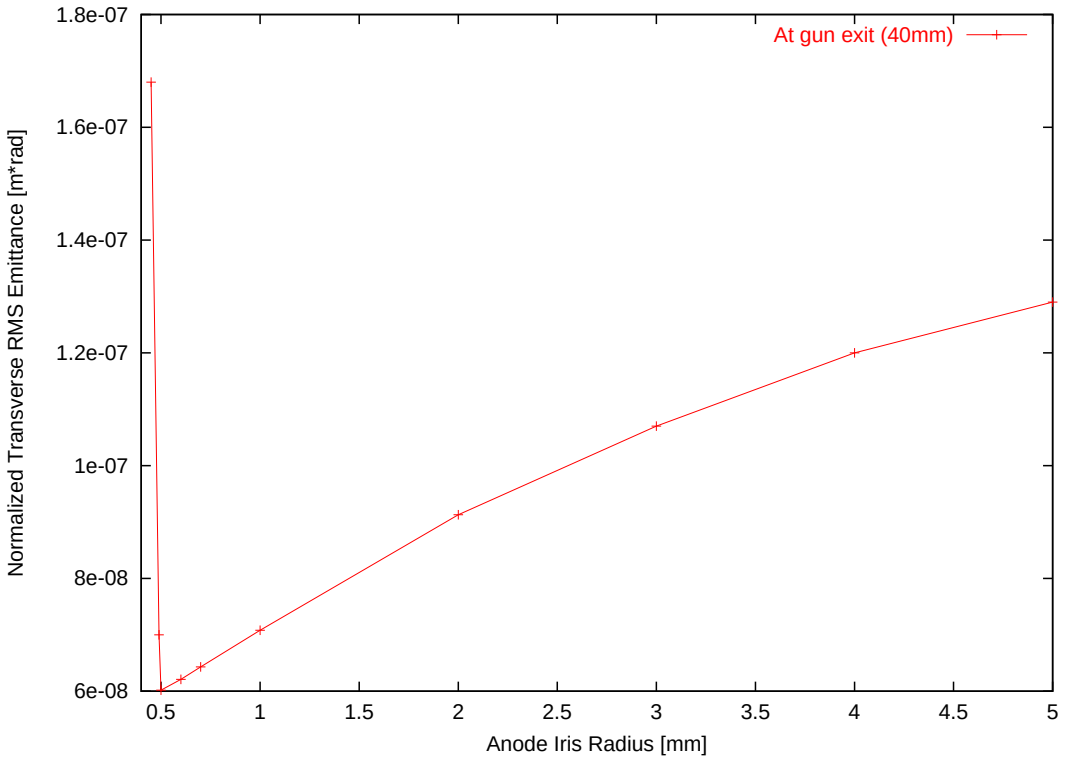

Figure 18: Emittance at the end of the gun depending on the radius of the anode iris. The sharp rise of emittance below a radius of 0.5 mm is due to the loss of particles on the anode iris for such small iris radii.

4 Scaling Laws and Extrapolation

As mentioned in section 3.4 the bunch chosen to perform these parameter studies was longitudinally Gaussian with a cut-off at $\pm 3\sigma_t$ where originally σ_t = 20 ps. However, this bunch length is actually about two orders of magnitude smaller than what is expected for the 100 keV test stand gun. The reason for this large discrepancy lies in the fact that the MAFIA data needed to evaluate the design can only be dumped at a certain time, but not at a certain location. If the bunch length were actually chosen such that σ_t = 1 ns and the dump time were chosen so that the head of the bunch had reached the end of the simulated beam line, the tail of the bunch would not yet have been emitted from the cathode! The number of macro-particles would be only a fraction of the total setting and the energy spread would be 100%. One would look at a bunch that has not yet fully been emitted nor accelerated!

In order to overcome this obstacle it was decided to use much shorter bunch lengths and at the same time reduce the contained charge to acquire the goal peak current of 100 mA. One possibility to check if the results obtained in such a manner can be extrapolated to the case where the test stand will operate is to compare simulations for reduced bunch charges with simulations for increased bunch lengths. In both cases the resulting charge density is the same so that one could simulate the realistic long bunch with a much shorter one by simply reducing the contained charge. Figure 19 shows the resulting emittance for simulated bunches where either the contained charge has been increased by a certain factor or the bunch length has been decreased by the same factor.

For low values of solenoid focussing, one can see very well that the simulated emittance differs relatively by a significant amount depending on variation of either charge or bunch length. Since both sets of data are derived from bunches with equal charge densities the difference in emittance could be explained by the bunch geometry: the simulated bunch is not disk-shaped or cigar-shaped, but rather in between these two extremes, where a slight change in the ratio between bunch length and radial bunch envelope has a large influence on the resulting space charge forces and thus on the obtained emittance. In the case of solenoid focussing at the nominal value or above, the difference between the emittance results ($< 10^{-8}$ m·rad) is hardly visible. In this manner the results can certainly be used to estimate an upper limit for the emittance.

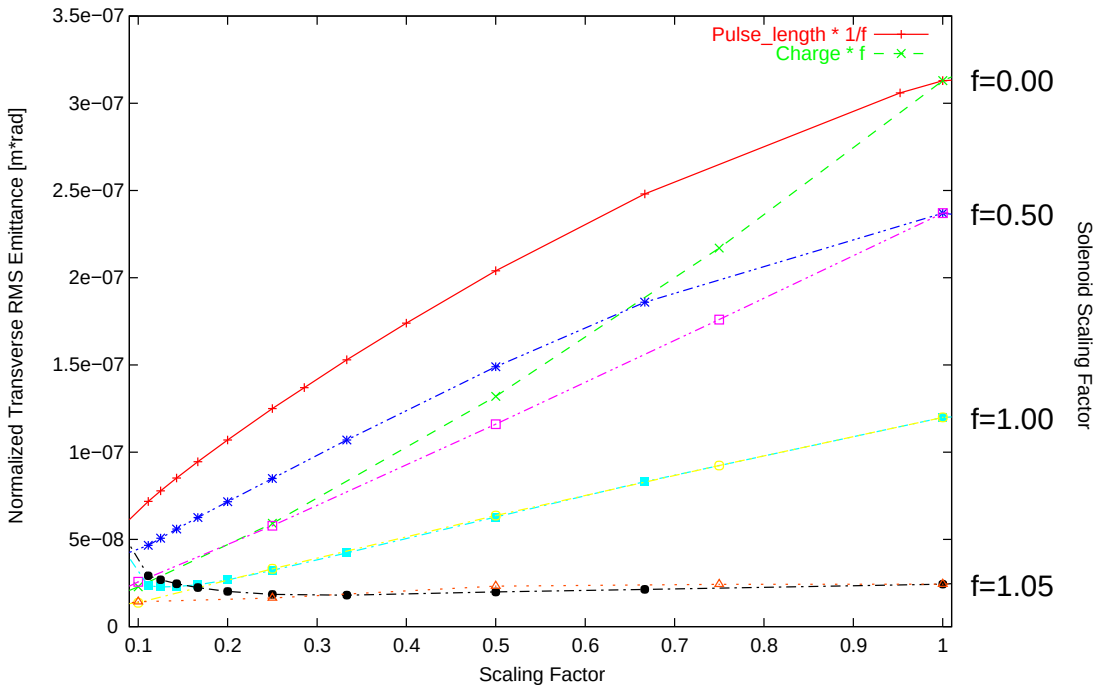

Figure 19: Four pairs (according to four different solenoid scalings) of curves for the emittance at the end of the beam line. For each pair the lower curve represents scaled charge while the upper curve represents scaled bunch length. A scaling of 1.0 refers to σ_t = 20 ps respectively Q = -5.0133·10^{-12} C (or a peak current of $\hat{I}$ = 100 mA); a solenoid scaling of 1.0 corresponds to a peak longitudinal magnetic field of $B_z \simeq 85$ mT.

5 Projected Emittance and Slice Emittance

In the scope of the LEG project a single-pass SASE FEL is considered as a source of short pulses of coherent 1Å X-rays [10]. In such a scheme it is found that the critical parameter in order to achieve high brightness laser pulses is the slice emittance rather than the projected emittance of the entire bunch [11]. MAFIA by itself delivers only the projected emittance of the bunch, but it can be forced to dump the radial and longitudinal phase space of all particles at a certain time t_0. As suggested in [12] one can approximate the slice emittance with the dumped phase space data.

Recall, when speaking of the normalized transverse RMS emittance one normally refers to the projected emittance (which is a property of one entire bunch) defined as:

$$\varepsilon = \sqrt{\langle r^2 \rangle \langle {p_r}^2 \rangle - \langle r\, p_r \rangle^2} \tag{4}$$

In monochromatic (the enegry spread σ_E/E in these simulation is always well below 1%) and paraxial (the beam divergence here is lower than 20 mrad) approximation one then can simplify:

$$\varepsilon = \gamma\beta \sqrt{\langle r^2 \rangle \langle r'^2 \rangle - \langle r\, r' \rangle^2} \tag{5}$$

From which one can derive the slice emittance (which depends on the location t_0 of the slice within the bunch and the width σ_t of the slice):

$$\varepsilon_{t_0} = \gamma\beta \sqrt{\langle r_{t_0}^2 \rangle \langle {r'}_{t_0}^2 \rangle - \langle r_{t_0}\, {r'}_{t_0} \rangle^2} \tag{6}$$

With slice means calculated according to:

$$\langle r_{t_0}^2 \rangle = \frac{1}{W_0} \sum_{i=1}^{N} {r_i}^2 \cdot w_{i,0} \tag{7}$$

Where a weighting function has been introduced:

$$w_{i,0} = e^{-\frac{(t_i - t_0)^2}{2\sigma_t^2}} = e^{-\frac{(z_i - z_0)^2}{2\beta^2 c^2 \sigma_z^2}} \qquad W_0 = \sum_{i=1}^{N} w_{i,0} \tag{8}$$

When performing these calculations the parameters (number of slices within the bunch, slice width σ_z) have to be chosen carefully due to the trade-off between numerical noise and possible resolution.

An example for such a slice emittance calculation is given in figure 20. As expected the slice emittances lie well below the projected emittance of the entire bunch. Also, one can see well that the slice emittance is larger at the ends than at the center of the bunch; this is what one would expect due to the fact that non-linear space charge forces (which blow up the emittance) are largest at the bunch ends.

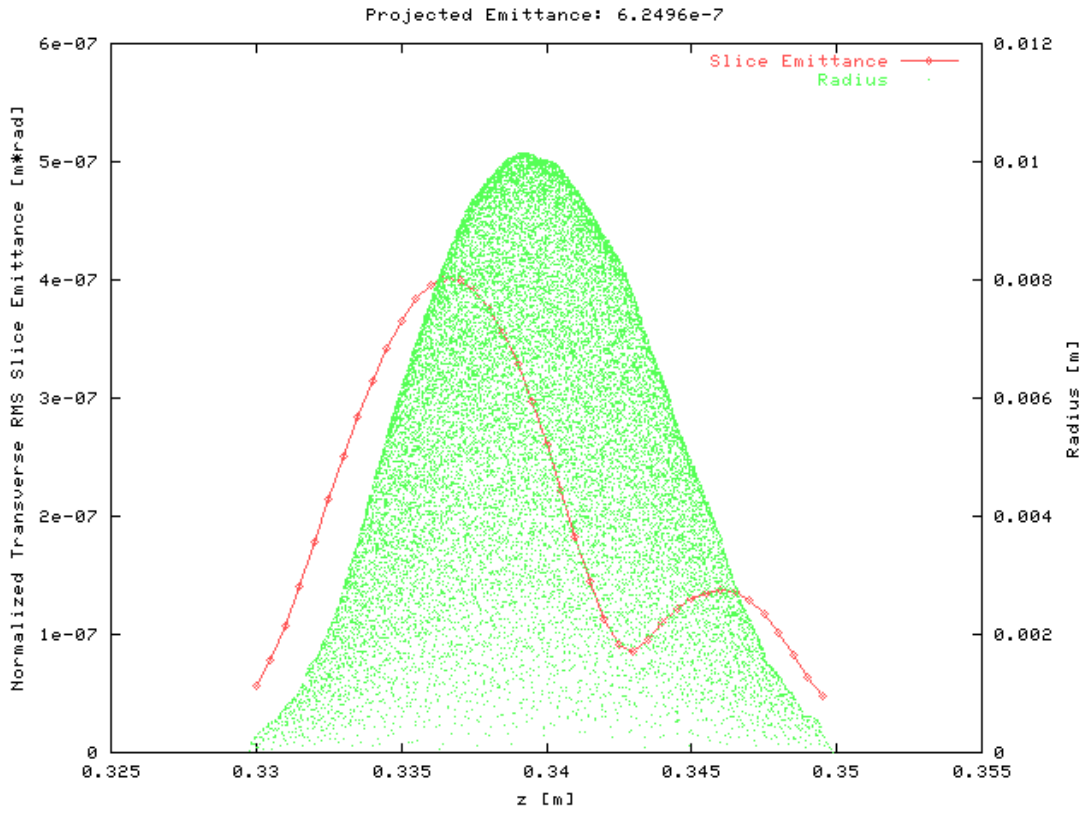

Figure 20: An example for the calculation of the slice emittance from dumped MAFIA phase space data. Each green dot represents a single macro-particle. The red curve is the calculated slice emittance (here we chose the slice width σ_z = 0.3 mm). The projected normalized transverse emittance of the entire bunch is $6.2496 \cdot 10^{-7}$ m·rad which is well above the values for the slice emittances.

References

[1] The Low Emittance Gun Project LEG at PSI, `http://leg.web.psi.ch`

[2] MAFIA 4 commercial particle tracking code, `http://www.cst.de`

[3] A. Streun, *Proposal for a FEA test gun*, internal note based on a meeting on Aug. 20, 2003

[4] M. Dehler, private communication

[5] M. v. Ardenne, *Tabellen der Elektronenphysik, Ionenphysik und Übermikroskopie*, Band II, 1956

[6] M. Paraliev, R. Ganter, M. Dehler, private communication at the LEG meeting, December 17, 2003

[7] J. R. Pierce, *Rectilinear Electron Flow in Beams*, Journal of Applied Physics **11**, 548, (1940)

[8] A. Streun, private communication about unpublished preliminary material

[9] B. E. Carlsten, *New Photoelectric Injector Design for the Los Alamos National Laboratory XUV FEL Accelerator*, Nuclear Instruments and Methods **A285**, 313, (1989)

[10] M. Pedrozzi et al., *Motivations and Limitations of the Low Emittance Gun*, PSI Scientific and Technical Report, Vol. VI, 2003

[11] R. Cee, M. Krassilnikov, S. Setzer, T. Weiland, *Beam Dynamics Simulations for the PITZ RF-Gun*, Proceedings of EPAC 2002, Paris, France

[12] A. Candel, M. Dehler, S. C. Leemann, *Electron Beam Dynamics Simulations for the Low Emittance Gun*, PSI Scientific and Technical Report, Vol. VI, 2003